

See discussions, stats, and author profiles for this publication at: <https://www.researchgate.net/publication/228799835>

Patterning on Self-Assembled Monolayers by Low-Energy Electron-Beam Irradiation and its Vertical Amplification with Atom Transfer Radical Polymerization

ARTICLE *in* LANGMUIR · MAY 2003

Impact Factor: 4.46 · DOI: 10.1021/la027055u

CITATIONS

33

READS

21

2 AUTHORS, INCLUDING:



Joon Won Park

Pohang University of Science and Technology

96 PUBLICATIONS 2,157 CITATIONS

SEE PROFILE

Patterning on Self-Assembled Monolayers by Low-Energy Electron-Beam Irradiation and its Vertical Amplification with Atom Transfer Radical Polymerization

Il Sang Maeng and Joon Won Park*

Center for Integrated Molecular Systems, Department of Chemistry, Division of Molecular and Life Sciences, Pohang University of Science and Technology, San 31 Hyoja-dong, Pohang 790-784, Korea

Received December 20, 2002.

In Final Form: February 23, 2003

Introduction

The electron-beam system has been used for many years to make the masks needed for optical lithography because of the high resolution offered by electron-beam tools. Because the wavelength of the electrons used in these tools is less than 0.1 nm, diffraction effects and the limits on optical exposure systems are not issues in electron-beam systems. Thus, there is no problem in the ability of the electron-beam tool to provide the resolution required for feature sizes. But the major drawback of the electron beam is the very low throughput compared to that of the current optical lithography method because the electron-beam tools essentially expose the resist by a serial process. The proximity effects are an additional significant issue associated with the electron-beam direct writing; the electrons striking the resist typically have an energy of 10–20 keV, travel distances greater than 1 μ m, and scatter so readily that exposure of the regions adjacent to the desired exposure areas occurs. Recently, a parallel-type patterning method has been devised as an approach to high-throughput electron-beam lithography, adopting new resist materials and mask designs.¹ Therefore, the electron-beam-lithography method has the advantage for high resolution and high throughput and now has been regarded as the next-generation lithography method that might replace the conventional UV lithography.

The radical-type polymerization method has been widely used for manufacturing various kinds of commercial products because of the stability of the radical species in the polymerization system compared with that in other types of polymerization systems and the applicability for the various kinds of monomers. Radical species are so reactive that control of the activity was considered very difficult, but recently, there were reports that it is possible to reduce the radical concentration in some systems for better control.² Atom transfer radical polymerization (ATRP) is one of these systems. Therefore, it is possible to prepare various kinds of block copolymers, such as diblock-, triblock-, and gradient-type copolymers and so on, with precise control featuring ATRP.³ In addition, it is possible to combine the method with other types of polymerization such as ring-opening metathesis polymerization or anion polymerization because there exists a functional group such as a halide at the end of the polymer chain, so many kinds of polymers that were thought to be

unable to prepared with other types of polymerization systems can be simply prepared with ATRP.⁴ There have been many reports on the preparation of “graft from” type polymer brushes with the ATRP method, manipulating its living nature and wide applicability to the various kinds of monomers.⁵ The reports showed that it was possible to control the surface property systematically by controlling the density of the initiator on the substrates or by selecting monomers. The polymer brush, especially, has the advantage over the spin-coated polymer layer in its stability against the solvents or the harsh conditions, such as high temperature, because of the stable covalent bond between the polymers and the substrates. These desirable traits have been manipulated in the areas of microelectronics and microfluidics.⁶

We prepared a self-assembled monolayer (SAM) of an ATRP initiator and irradiated a low-energy electron beam onto it through a mask. The energy of the electron beam was so low that the proximity effect of the electron beam was minimized. And the patterned monolayer was amplified vertically with ATRP; in particular, the Cu(I) catalyst and tris[2-(dimethylamino)ethyl]amine (Me₆TREN) ligand are employed for the polymerization at room temperature.⁷ At a higher temperature, the radical species can also be generated thermally in the solution phase, so polymers produced in the latter phase tend to adsorb physically on the substrate surface. These polymers should be removed with a tedious extraction process, but there is not such a problem with the room-temperature ATRP. The two types of monomers were employed for the successful amplification, and effective wet-etching resistance leading to a high aspect ratio was observed.

Experimental Section

General Procedures. The silane coupling agent, (3-amino-propyl)diethoxymethylsilane, was purchased from Gelest, Inc. 1-Ethyl-3-(dimethylamino)propylcarbodiimide (EDAC), pentafluorophenol (PFP), styrene, methyl methacrylate (MMA), copper(I) bromide, a 48% HF solution, and ammonium fluoride

* Corresponding author. Fax: (+82)-54-279-8365. E-mail: jwpark@postech.ac.kr.

(1) Harriott, L. R. *IEEE Spectrum* **1999**, 41.

(2) General reviews on living radical polymerization: (a) Hawker, C. J. *Acc. Chem. Res.* **1997**, 30, 373. (b) Xia, J.; Matyjaszewski, K. *Chem. Rev.* **2001**, 101, 2921. (c) Kamigaito, M.; Ando, T.; Sawamoto, M. *Chem. Rev.* **2001**, 101, 3689.

(3) (a) Patten, T. E.; Xia, J.; Abernathyl, T.; Matyjaszewski, K. *Science* **1996**, 272, 866. (b) Patten, T. E.; Matyjaszewski, K. *Acc. Chem. Res.* **1999**, 32, 895. (c) Liu, S.; Sen, A. *Macromolecules* **2000**, 33, 5106. (d) Borner, H. G.; Beers, K.; Matyjaszewski, K.; Sheiko, S. S.; Moller, M. *Macromolecules* **2001**, 34, 4375. (e) Shinoda, H.; Matyjaszewski, K. *Macromolecules* **2001**, 34, 6243. (f) Liu, S.; Weaver, J. V. M.; Tang, Y.; Billingham, N. C.; Armes, S. P.; Tribe, K. *Macromolecules* **2002**, 35, 6121. (g) Hester, J. F.; Banerjee, P.; Won, Y. Y.; Akthakul, A.; Acar, M. H.; Mayes, A. M. *Macromolecules* **2002**, 35, 7652. (h) Lu, S.; Fan, Q. L.; Liu, S. Y.; Chua, S. J.; Huang, W. *Macromolecules* **2002**, 35, 9875. (4) (a) Coca, S.; Paik, H.; Matyjaszewski, K. *Macromolecules* **1997**, 30, 6513. (b) Zhao, B.; Brittain, W. J. *J. Am. Chem. Soc.* **1999**, 121, 3557. (c) Bielawski, C. W.; Morita, T.; Grubbs, R. H. *Macromolecules* **2000**, 33, 678. (d) Tong, J. D.; Zhou, C.; Ni, S.; Winnik, M. A. *Macromolecules* **2001**, 34, 696. (e) Heise, A.; Trollsas, M.; Magbitang, T.; Hedrick, J. L.; Frank, C. W.; Miller, R. D. *Macromolecules* **2001**, 34, 2798. (f) Feng, X. S.; Pan, C. Y. *Macromolecules* **2002**, 35, 2084. (5) (a) Hussemann, M.; Malmstrom, E. E.; Hawker, C. J. *Macromolecules* **1999**, 32, 1424. (b) Matyjaszewski, K.; Hiller, J.; Pakula, T. *Macromolecules* **1999**, 32, 8716. (c) Fukuda, T. *Macromolecules* **2000**, 33, 8716. (d) Iyoda, T. *Macromolecules* **2001**, 34, 1837. (e) Costa, R. O. R.; Vasconcelos, W. L.; Tamaki, R.; Laine, R. M. *Macromolecules* **2001**, 34, 5398. (f) Cheng, G.; Boker, A.; Zhang, M.; Krausch, G.; Muller, A. H. E. *Macromolecules* **2001**, 34, 6883. (g) Zheng, G.; Stover, H. D. H. *Macromolecules* **2002**, 35, 6828. (h) Wang, J. Y.; Chen, W.; Liu, A. H.; Lu, G.; Zhang, G.; Zhang, J. H.; Yang, B. *J. Am. Chem. Soc.* **2002**, 124, 13358. (6) (a) Huang, X.; Wirth, M. J. *Anal. Chem.* **1997**, 69, 4577–4580. (b) Huang, X.; Donesk, L. J.; Wirth, M. J. *Anal. Chem.* **1998**, 70, 4023–4029. (c) Hussemann, M.; Morrison, M.; Hawker, C. J. *J. Am. Chem. Soc.* **2000**, 122, 1844. (d) Hyun, J.; Chilkoti, A. *Macromolecules* **2001**, 34, 5644. (7) Baker, G. L. *J. Am. Chem. Soc.* **2000**, 122, 7616.

Scheme 1. Preparation of a Patterned Polymer Brush by Low-Energy Electron-Beam Irradiation through a Mask

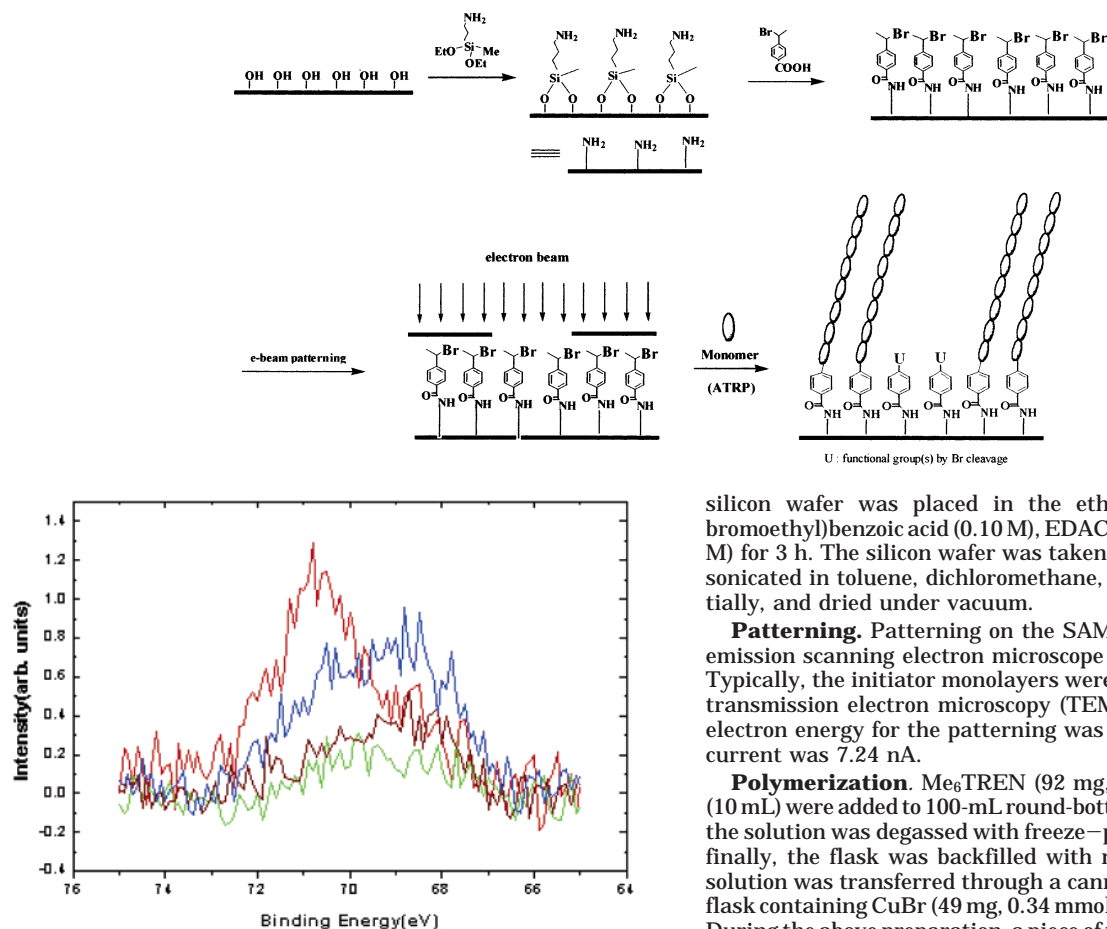


Figure 1. X-ray photoelectron spectra before and after the electron-beam irradiation (0.50 keV). The light-red line is the spectrum without electron-beam irradiation, the blue line is the spectrum with electron-beam irradiation for 2.0 min, the dark-red line is the spectrum with electron-beam irradiation for 4.0 min, and the green line is the spectrum with electron-beam irradiation for 6.0 min.

were purchased from the Aldrich Chemical Co. Styrene and MMA were purified with CaH_2 and vacuum-transferred before use. 4-(1-Bromoethyl)benzoic acid was purchased from Lancaster Synthesis. Me_6TREN was prepared by literature procedures.⁸ UV-grade fused-silica plates were purchased from the CVI Laser Co. The polished, prime Si(100) wafers (dopant, phosphorus; resistivity, 1.5–2.1 $\Omega\cdot\text{cm}$) were purchased from MEMC Electronic Materials, Inc. UV–visible spectra were recorded on a Hewlett-Packard diode-array 8453 spectrophotometer. Deionized water (18 $\text{M}\Omega\cdot\text{cm}$) was obtained by passing distilled water through a Barnstead E-pure 3-Module system. The facilities of Pohang Accelerator Laboratory (Pohang, Korea) were used for the cleavage process and X-ray photoelectron spectroscopy (XPS) analysis of the bromo-substituted benzamide monolayer. Electron binding energies were calibrated against the Si(2p) emission at $E_b = 99.3$ eV. Images and cross-sectional profiles of the polymer films and etched silicon wafers were obtained by atomic force microscopy (AFM) with an atomic force microscope (Digital Instruments NanoScope III) operating in a tapping mode. Samples were scanned under ambient conditions using a cantilever made from silicon nitride.

Preparation of the Initiator Monolayer. The aminosilylated monolayers were prepared by treating the silicon wafer with (3-aminopropyl)diethoxymethylsilane.⁹ The aminosilylated

silicon wafer was placed in the ethanol solution of 4-(1-bromoethyl)benzoic acid (0.10 M), EDAC (0.10 M), and PFP (0.20 M) for 3 h. The silicon wafer was taken out of the solution and sonicated in toluene, dichloromethane, and methanol, sequentially, and dried under vacuum.

Patterning. Patterning on the SAM was done with a field emission scanning electron microscope (FESEM; JEOL 6320). Typically, the initiator monolayers were scanned for 1 h with a transmission electron microscopy (TEM) grid as a mask. The electron energy for the patterning was 1.0 keV, and the beam current was 7.24 nA.

Polymerization. Me_6TREN (92 mg, 0.40 mmol) and MMA (10 mL) were added to 100-mL round-bottom flask; subsequently, the solution was degassed with freeze–pump–thaw cycles; and finally, the flask was backfilled with nitrogen. The resulting solution was transferred through a cannula to a nitrogen-filled flask containing CuBr (49 mg, 0.34 mmol) and stirred for 20 min. During the above preparation, a piece of the prepatterned silicon wafer was placed in the two-neck round-bottom flask, and the flask was evacuated and backfilled with nitrogen. To this flask was again transferred the above solution through a cannula, and the flask was placed at room temperature. After several hours, the substrate was removed from the flask; washed with chloroform; and sonicated in toluene, dichloromethane, and methanol in a sequential manner. The conditions for the polymerization of styrene were the same as those of MMA, except that the polymerization temperature was 50 $^\circ\text{C}$.

Etching. Ammonium fluoride (8.0 g) was dissolved in deionized water (12 mL), a 48% HF solution (2.5 mL) was added, and the resulting solution was stirred for 5 min. The patterned and polymerized silicon wafer was dipped in the solution for 3 min. The etched silicon substrate was washed with water and vacuum-dried. To check the defects, if any, after the etching, the polymer layer was removed by piranha-solution treatment (7:3 $\text{H}_2\text{SO}_4/\text{H}_2\text{O}_2$).

Results and Discussion

The bromo-substituted aromatic amide monolayer used in this study was prepared by the treatment of aminosilylated substrates with the relevant aromatic acid (Scheme 1). The physical change of the substrate at each step was characterized with a UV–vis spectrometer and ellipsometer. An absorption peak at 243 nm arising from the aromatic group appeared in the UV–vis spectrum after the amide bond formation, and the thickness of the monolayer also increased from 12 to 17 Å (increment of about 5 Å). The intensity of the absorption peak for aromatic group did not increase noticeably after 3 h. The amide bond formation of the EDAC–PFP system was more efficient at room temperature than that at a higher temperature, presumably because of the low thermal stability of the EDAC–PFP system.

(8) Matyjaszewski, K.; Patten, T. E.; Xia, J. *J. Am. Chem. Soc.* **1997**, *119*, 674.

(9) Moon, J. H.; La, Y.; Park, J. W. *Langmuir* **2000**, *16*, 2981.

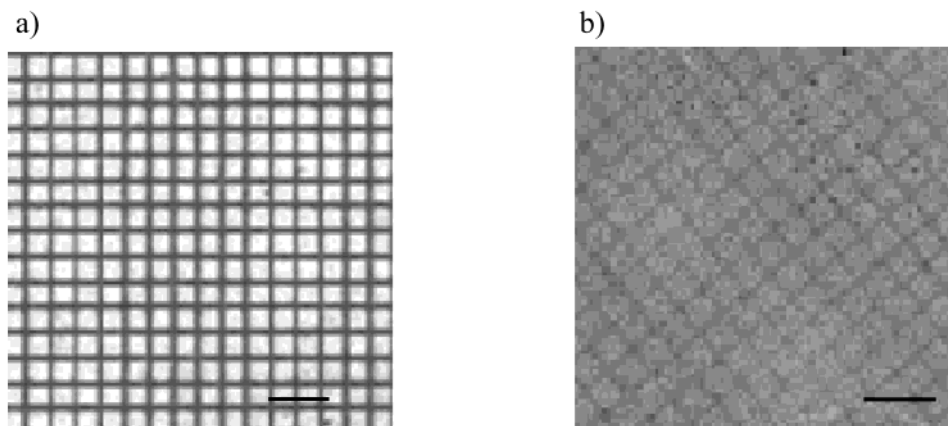


Figure 2. FESEM images of the patterned PMMA brush fabricated with different electron-beam energies: (a) electron-beam energy of 1.0 keV and (b) electron-beam energy of 30 keV. The length of the scale bars is 50 μm .

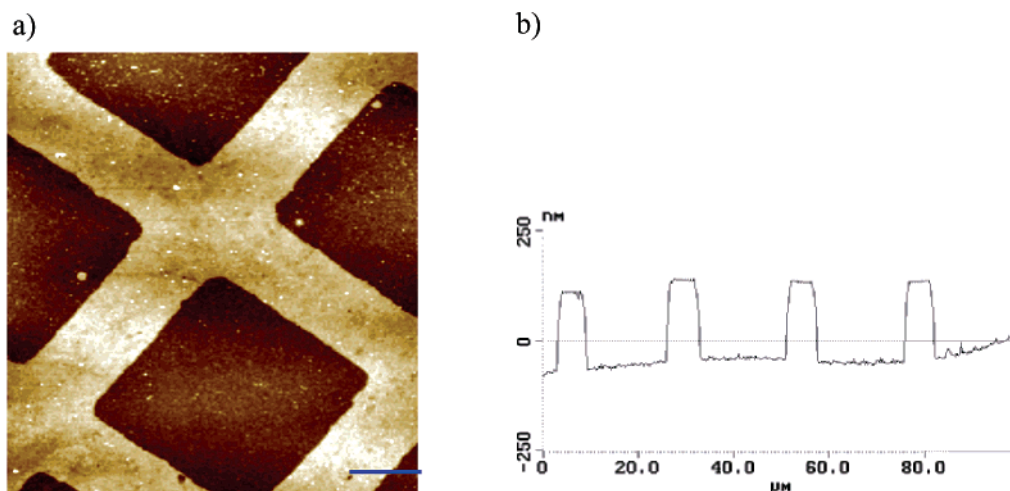


Figure 3. (a) AFM image of the patterned PS brush. The length of the scale bar is 5.0 μm . (b) AFM height profile of the wet-etched pattern.

A synchrotron radiation facility was utilized for the XPS analysis of the monolayer and the kinetics study on the bromide cleavage. The survey spectrum of the bromo-substituted benzamide monolayer obtained with 830-eV irradiation showed bands from the O(1s), N(1s), C(1s), Si(2s), Si(2p), and Br(3d) levels. The positions of these bands coincide well with the literature values. The Br(3d) binding-energy region was carefully scrutinized by the irradiation of 400-eV X-rays to measure the rate of bromide cleavage quantitatively. Figure 1 shows the Br(3d) binding-energy region (65–75 eV) of the 4-(1-bromoethyl)-benzamide monolayer. The red line corresponds to the band before the electron-beam irradiation (0.50 keV; beam-current density, 0.32 $\mu\text{A}/\text{cm}^2$), and the green line is the band observed after the electron-beam irradiation for 6.0 min. The Br(3d) peak for 4-(1-bromoethyl)benzamide group at 70.8 eV decreases with the electron-beam irradiation, a small peak at 68.8 eV appears concomitantly, and both disappear almost completely in 6.0 min. There were some reports that the primary event in the electron-irradiation-induced processes could be the cleavage of the C–Br and C–H bonds for several aliphatic and aromatic SAMs, with concomitant cross-linking of the carbon chains,¹⁰ so we assume that the transient peak would be from a bromophenyl intermediate. The transfer of the bromine radical to the benzene ring is most likely to happen at the initial stage. Eventually, the bromide was

eliminated from the system, leading to the permanent deactivation of the irradiated initiator. A contrasting feature, no noticeable changes in the shapes and intensities of the C(1s) and O(1s) peaks during the cleavage process, was observed.

Patterning on the SAM was performed by electron irradiation using FESEM. The employed electron energy was 1.0 keV, and the beam current was 7.24 nA. At energies lower than 1.0 keV, the beam current was so low that effective patterning of the initiator layer required too much time. At the energy of 1.0 keV, the beam current was sufficient to make a pattern in 30 min, but the differentiated amplification was not effective. Therefore, 1 h was found to be the optimized irradiation time for the patterning and the selective vertical amplification through ATRP of styrene or MMA. In particular, the deleterious proximity effect of the electron beam incurred by scattering was minimized because the low electron energy was used for the patterning. In Figure 2, the dark line of the FESEM image is the poly(methyl methacrylate) (PMMA) brush, and the bright square is the irradiated region. As in Figure 2a, the high contrast between the unirradiated region and the irradiated one was observed when an electron-beam energy of 1.0 keV was employed. However, at 30 keV the contrast is poor because the amount of tethered polymer is low, even within the unirradiated regions (Figure 2b). It is believed that the scattered electrons at the higher energy traveled farther, resulting in the cleavage of the halide group located under the mask.

(10) (a) Ech, W.; Stadler, V.; Grunze, M. *Adv. Mater.* **2000**, *12*, 805.
(b) Golzhauser, A.; Eck, W.; Grunze, M. *Adv. Mater.* **2001**, *13*, 806.

After the patterning, polymer chains of MMA or styrene were grown with a CuBr/Me₆TREN catalytic system at room temperature or 50 °C, respectively. The physisorption of the polymer grown in the solution phase was not significant for the two particular cases. Therefore, light sonication treatment in organic solvents was good enough to eliminate the minor polymer aggregates adsorbed on the surface. The resulting surface was then characterized with AFM. Figure 3a shows an AFM image of the patterned polystyrene (PS) brush with a line width of 6.5 μm. The light line corresponds to the PS brush, and the dark square is the irradiated part. The thickness of the PS layer was characterized to be about 300 Å, and the surface roughness was about 15 Å. For the PMMA brush, the typical thickness was 250 Å, and the surface roughness was about 10 Å.

The patterned PS and PMMA brushes were examined for use as the etch mask. For this particular test, a piece of silicon wafer on which the oxide layer thickness was 0.20 μm was employed. After the formation of the patterned PS or PMMA brush, the wafer was etched with a buffered HF solution for 3 min, and the etched layer was finally characterized with AFM after the polymeric layer was removed. Figure 3b is an AFM height profile of the patterned silicon oxide layer when the PS brush was used as the mask. In the figure, the depth of the etched silicon oxide layer is as deep as about 2.0×10^3 Å, which shows the oxide layer is fully etched during the 3 min. The height profile with the high aspect ratio demonstrates that the polymer brush is very stable against the buffered HF

solution. The PMMA brush is also resistant to the buffered HF solution, and the resulting aspect ratio is almost the same as that of the PS brush.

Even though a TEM grid with submicrometer resolution is not available now, it is expected to produce a pattern with nanometer resolution in a parallel manner as long as a relevant mask is in hand.

Conclusion

A SAM of an initiator for ATRP was patterned by low-energy electron-beam irradiation, and the pattern was vertically amplified and transformed into patterned PS or PMMA brushes at mild conditions. Finally, selective wet etching was demonstrated with the patterned and amplified substrates. Higher resolution was observed for this particular system because of the low-energy nature of the employed electron beam. Because the amplification with ATRP is applicable to the various types of monomers, tailoring the chemical and physical properties of the microstructure and nanostructure is conceivable.

Acknowledgment. Student fellowships of Brain Korea 21 are gratefully acknowledged, and this work is also supported by the Korea Science and Engineering Foundation through the Center for Integrated Molecular Systems. We thank Mr. T.-H. Kang and Mr. K.-W. Ihm (PLS) for help with the XPS experiments.

LA027055U